Contribution from the Department of Chemistry,
The University of Western Ontario, London, Ontario, Canada N6A 5B7

Reactions of H_2S and H_2Se with Coordinatively Unsaturated Clusters: Structure of $[Pt_3H(\mu_3\text{-}S)(\mu\text{-}Ph_2PCH_2PPh_2)_3][BPh_4]$

Michael C. Jennings, Nicholas C. Payne,* and Richard J. Puddephatt*

Received May 11, 1987

Reactions of H_2E with $[M_3(\mu_3\text{-CO})(\mu\text{-dppm})_3][PF_6]_2$ (**1**, M = Pt; **2**, M = Pd) give the complexes $[M_3H(\mu_3\text{-E})(\mu\text{-dppm})_3][PF_6]$ (**3**, M = Pt, E = S; **4**, M = Pt, E = Se; **5**, M = Pd, E = S). The platinum complexes **3** and **4** are thermally stable, but the palladium complex **5**, which is apparently the first hydridopalladium cluster complex, reacts readily with excess H_2S or with $CHCl_3$ to give $[Pd_3X(\mu_3\text{-S})(\mu\text{-dppm})_3][PF_6]$ (**6**, X = SH; **7**, X = Cl). The new complexes are 46e clusters that contain only one metal–metal bond. They are characterized by NMR, IR, and FAB MS methods. The complexes undergo inversion of the $M_3(\mu_3\text{-E})$ groups as determined by variable-temperature NMR spectroscopy, and trends in the activation energies for inversion are discussed. The structure of $[Pt_3H(\mu_3\text{-S})(\mu\text{-dppm})_3][BPh_4]$ has been determined by X-ray crystallography. The salt crystallizes with four formula units in space group $P2_1/c$, with cell dimensions $a = 11.338$ (1) Å, $b = 17.303$ (2) Å, $c = 42.957$ (3) Å, and $\beta = 90.30$ (1)°. The analysis converged to an R factor of 0.0429 for 303 variables and 8258 independent observations with $I > 3\sigma(I)$. The cation contains a triangle of platinum atoms linked by dppm ligands and a triply bridging sulfur atom. Only the Pt(1)–Pt(3) distance of 2.597 (4) Å is typical of a Pt–Pt single bond. The terminal hydride ligand was located and refined (Pt(2)–H = 2.15 (8) Å; S–Pt(2)–H = 179 (2)°).

Introduction

The strong adsorption of sulfur to various transition metals can be responsible for the poisoning of heterogeneous catalysts and has led to several studies of the reactions of H_2S on metal surfaces.[1-8] In the case of the platinum(111) surface, the H_2S reacts to evolve hydrogen and leave a sulfide coat on the surface.[1-3,5,9] LEED analysis shows this coat to consist of $Pt_3(\mu_3\text{-S})$ units.[9]

In order to model the poisoning of platinum surfaces by hydrogen sulfide, the reactions of H_2S with the coordinatively unsaturated cluster cations $[M_3(\mu_3\text{-CO})(\mu\text{-dppm})_3]^{2+}$ (**1**, M = Pt;[10] **2**, M = Pd[11]) have been studied. In these complexes each metal atom is coordinatively unsaturated,[12] and the chemistry of the M_3 triangle may therefore be expected to mimic chemistry at a triangular unit of the M(111) surface.[13] The three bridging bis(diphenylphosphino)methane (dppm) ligands should serve to maintain the integrity of the cluster throughout the reaction, and avoid the common problem of cluster fragmentation.[13,14] Previous studies have established the validity of this approach,[15,16] for example in the oxidative addition of thiocyanate to **2** and in the addition of alkynes to the related cluster $[Pt_3(\mu_3\text{-H})(\mu\text{-dppm})_3]^+$. These reactions occur with cleavage of metal–metal bonds, whereas addition of Lewis bases such as CO occurs without such cleavage.[15,16] A preliminary account of parts of the present work has been published.[17]

(1) Koestner, R. J.; Salmeron, M.; Kollin, E. B.; Gland, J. L. *Surf. Sci.* **1986**, *172*, 668.
(2) Protopopoff, E.; Marcus, P. *Surf. Sci.* **1986**, *169*, L237.
(3) Kelemen, S. R.; Fischer, T. E.; Schwarz, J. A. *Surf. Sci.* **1979**, *81*, 440.
(4) Wong, P. C.; Zhou, M. Y.; Hui, K. C.; Mitchell, K. A. R. *Surf. Sci.* **1985**, *163*, 172.
(5) Billy, J.; Abon, M. *Surf. Sci.* **1984**, *146*, L525.
(6) Fischer, T. E.; Keleman, S. R. *Surf. Sci.* **1977**, *69*, 1.
(7) Trenary, M.; Uram, K. J.; Yates, J. T., Jr. *Surf. Sci.* **1985**, *157*, 512.
(8) Bonzel, H. P.; Ku, R. *J. Chem. Phys.* **1973**, *58*, 4617.
(9) Hayek, K.; Glassl, H.; Gutmann, A.; Leonhard, H.; Prutton, M.; Tear, S. P.; Welton-Cook, M. R. *Surf. Sci.* **1985**, *152/153*, 419.
(10) Ferguson, G.; Lloyd, B. R.; Puddephatt, R. J. *Organometallics* **1986**, *5*, 344.
(11) Manojlović-Muir, L.; Muir, K. W.; Lloyd, B. R.; Puddephatt, R. J. *J. Chem. Soc., Chem. Commun.* **1983**, 1336.
(12) Mealli, C. *J. Am. Chem. Soc.* **1985**, *107*, 2245.
(13) Muetterties, E. L. *Catal. Rev.—Sci. Eng.* **1981**, *23*, 69.
(14) (a) Vahrenkamp, H. *Adv. Organomet. Chem.* **1983**, *22*, 169. (b) Adams, R. D.; Horváth, I. T. *Prog. Inorg. Chem.* **1985**, *33*, 127.
(15) Rashidi, M.; Puddephatt, R. J. *J. Am. Chem. Soc.* **1986**, *108*, 7111. Lloyd, B. R.; Bradford, A.; Puddephatt, R. J. *Organometallics* **1987**, *6*, 424. Ling, S. S. M.; Hadj-Bagheri, N.; Manojlović-Muir, L.; Muir, K. W.; Puddephatt, R. J. *Inorg. Chem.* **1987**, *26*, 231.
(16) Ferguson, G.; Lloyd, B. R.; Manojlović-Muir, L.; Muir, K. W.; Puddephatt, R. J. *Inorg. Chem.* **1986**, *25*, 4190.
(17) Jennings, M. C.; Payne, N. C.; Puddephatt, R. J. *J. Chem. Soc., Chem. Commun.* **1986**, 1809.

Table I. NMR Data (J in Hz)

	complex				
	3	4	5	6	7
δ(M–H)	−9.24	−8.48	−8.11	−2.16[d]	...
^1J(PtH)	1106	1190	...	...	...
^2J(P^{a}H)	13.5	12.3	6.9	8[d]	...
^4J(P^{b}H)	2.9	2.3	2.6	...	...
δ(C^{1}H$_2$)	4.0	4.9, 5.1	3.7	3.7	3.7
δ(C^{2}H$_2$)	5.6	3.6	5.1	5.1	5.2
δ(P^a)	22.8	21.9	29.8[b]	22.8	19.9
^1H(PtP^a)	2992	2957	...	...	...
^2J(P^{a}P^b)	27	27	50	35[e]	35[e]
δ(P^b)	2.6	4.5	2.5	−2.1	−2.3
^1J(PtP^b)	3110	3044	...	...	...
^2J(PtP^b)	181	180	...	...	...
^3J(P^{b}P^b)	161	174			
δ(P^c)	−15.1	−24.7	−8.5[c]	−7.0[f]	−6.8[f]
^1J(PtP^c)	3840	3980	...	...	...
δ(Pt^1)	−3181	−3288[a]	...	...	...
δ(Pt^2)	−3172	−3139	...	...	...
^1J(Pt^{2}Pt^2)	2620	2815			

[a] ^1J(PtSe) = 460 Hz. [b] ^4J(P^{a}P^b) = 40, ^4J(P^{a}P^c) = 4 Hz. [c] ^2J(P^{b}P^c) = 7 Hz. [d] PdS*H*; ^3J(PH) = 8 Hz. [e] ^4J(P^{a}P^b) = 35, ^4J(P^{a}P^c) = 6 Hz. [f] ^2J(P^{b}P^c) = 8 Hz.

Results

The major chemical results are shown in eq 1 (PP = dppm = $Ph_2PCH_2PPh_2$).

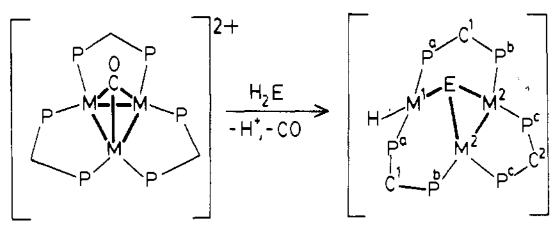

(1)

1, M = Pt
2, M = Pd

3, M = Pt, E = S
4, M = Pt, E = Se
5, M = Pd, E = S

The platinum complexes **3** and **4** could be prepared as stable yellow compounds by reaction of **1** with H_2S or H_2Se respectively at room temperature. An attempt was made to detect reaction intermediates by treating a solution of **1** with H_2S at −78 °C in an NMR tube, but the reaction was found to be complete at this temperature before a spectrum could be recorded. The reaction of the palladium complex **2** with H_2S was carried out at −78 °C and product **5** was isolated at low temperature, in order to avoid

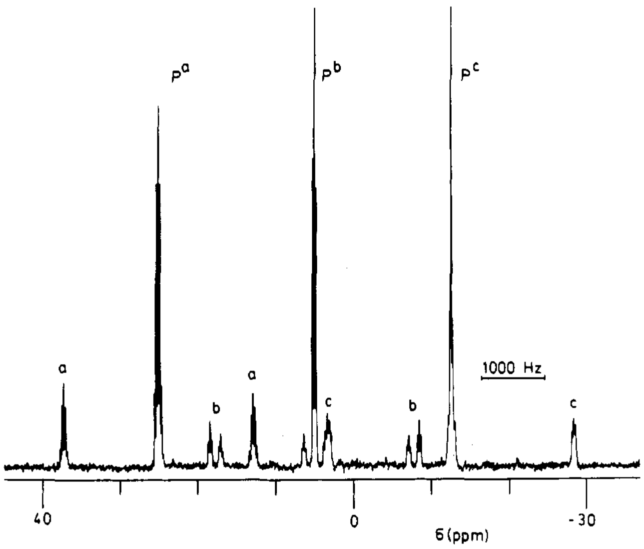

Figure 1. ^{31}P NMR spectrum (121.5 MHz) of complex **3**.

further reaction with H_2S. The hydridopalladium cluster **5** is apparently the first such compound to be reported. It is, like mononuclear palladium hydrides, of low thermal stability. If the synthesis in acetone solution was carried out at room temperature, a product tentatively formulated as $[Pd_3(SH)(\mu_3\text{-}S)(\mu\text{-}dppm)_3][PF_6]$ (**6**) was formed, and if the reaction was carried out in chloroform solution, the product was $[Pd_3Cl(\mu_3\text{-}S)(\mu\text{-}dppm)_3][PF_6]$ (**7**). These are evidently formed by reaction of the Pd–H group of complex **5** with either excess H_2S or with the chlorinated solvent. It has been shown previously[17] that the PtH bond of $[Pt_3H(\mu_3\text{-}SPh)(\mu\text{-}dppm)_3]^{2+}$ reacts with PhSH to give hydrogen and $[Pt_3(SPh)(\mu_3\text{-}SPh)(\mu\text{-}dppm)_3]^{2+}$, but the PdH bond of **5** is much more reactive. The palladium complexes failed to give good analytical data. In the case of **5** this was due to its thermal instability, but for **6** and **7** it appeared to be due to formation of elemental sulfur that could not be separated.

Characterization by Spectroscopic Methods. The structure of **3** was determined crystallographically (see below) and the other complexes **4–7** were characterized by using multinuclear NMR, IR, and FAB MS techniques.

The ^1H NMR spectra of **3–5** each contained a characteristic metal hydride resonance (Table I). The order of MH bond strengths appears to be **4** > **3** > **5**. For the platinum hydrides values of ^1J(PtH) for **4** and **3** were 1190 and 1106 Hz, respectively, suggesting a higher trans influence for μ_3-S over μ_3-Se.[18] Similarly, the ν(MH) values from the IR spectra followed the sequence **4** (2105 cm^{-1}) > **3** (2089 cm^{-1}) > **5** (1910 cm^{-1}). The low ν(PdH) value for **5** is consistent with the high reactivity of the PdH group.

The major evidence for the SH group in **6** was the observation of a characteristic SH resonance in the ^1H NMR spectrum at δ −2.6, which appeared as a triplet due to coupling to the neighboring ^{31}P atoms. The spectrum was reproducible.

The ^{31}P NMR spectra (e.g. Figure 1) of complexes **3–7** can be analyzed in terms of an $(AMX)_2$ spin system due to coupling between nonequivalent phosphorus atoms P^a, P^b, and P^c (see eq 1). The spectra of the palladium complexes were similar to those of $[Pd_3(CN)(\mu_3\text{-}S)(\mu\text{-}dppm)_3]^+$, which has been discussed earlier.[16] The spectra of the platinum complexes were considerably more complex, due to the presence of the isotopomers I–IV below, for which only the platinum atoms are shown, with natural abundances given below:

I	IIa	IIb	IIIa	IIIb	IV
Pt^1	Pt*	Pt	Pt*	Pt	Pt*
Pt^2–Pt^2	Pt–Pt	Pt*–Pt	Pt*–Pt	Pt*–Pt*	Pt*–Pt*
29.6%	14.8%	29.6%	14.8%	7.4%	3.7%

(18) Appleton, T. A.; Clark, H. C.; Manzer, L. E. *Coord. Chem. Rev.* **1973**, *10*, 335.

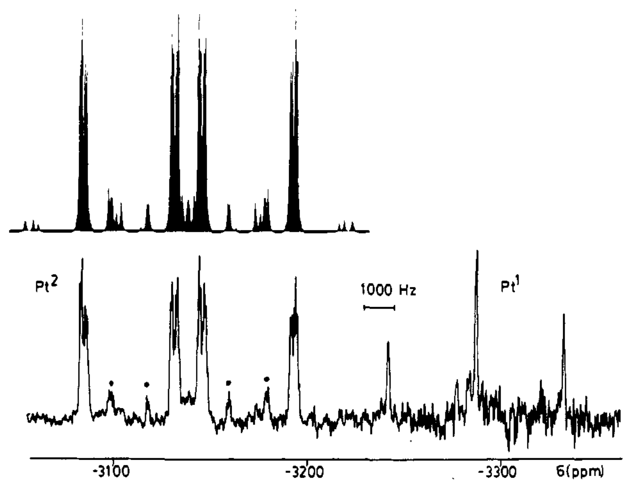

Figure 2. ^{195}Pt NMR spectrum (64.3 MHz) of complex **4**. A simulation of the Pt^2 resonance is shown above.

Table II. Activation Energies for Sulfur or Selenium Inversion

complex $[M_3X(\mu_3\text{-}E)(\mu\text{-}dppm)_3]^+$ M	X	E	ΔG^*, kJ mol^{-1}
Pt	H	S	54
Pt	H	Se	>65
Pd	H	S	48
Pd	CN	S	47[a]
Pd	SH	S	44
Pd	Cl	S	44.5

[a] From ref 16. Estimated errors ±2 kJ mol^{-1}.

Isotopomer I gives spectra analogous to those of the palladium complexes, but the more complex spectra of the other isotopomers are superimposed (Pt* represents ^{195}Pt). The situation is simplified to some extent because coupling between Pt^1 and Pt^2 (or phosphorus atoms bound to Pt^2) is negligibly small. Hence, the spectra can be rationalized in terms of whether Pt^1 is spin active (IIa, IIIa, IV) or not (I, IIb, IIIb) and whether the $Pt_2{}^2$ unit contains zero (I, IIa), one (IIb, IIIa), or two (IIIb, IV) ^{195}Pt atoms.

For isotopomers IIb and IIIa, the resonances due to the P^b atoms (eq 1) were of interest. Both couplings $^1J(Pt^2P^b)$ and $^2J(Pt^2P^b)$ were clearly resolved, and each contained an extra doublet splitting due to $^3J(P^bP^{b'})$. The observation of long range couplings ^2J(PtP) and ^3J(PP) is a characteristic of approximately linear P–Pt–Pt–P units and is a very useful criterion for the presence of such units.[10,15,19]

For isotopomers IIIb and IV the spin system is more complex, but simulation of the ^{31}P and ^{195}Pt NMR spectrum[20] gives a value for the coupling $^1J(Pt^2Pt^2)$ = 2620 Hz for **3** and 2815 Hz for **4**.

The ^{195}Pt NMR spectra consist largely of a triplet for Pt^1 and a doublet of doublets for Pt^2 due to ^1J(PtP) coupling (Figure 2). However, the more complex spin systems of IIIb and IV[20] again lead to further fine structure in the signal for Pt^2, and simulation can give $^1J(Pt^2Pt^2)$ (Figure 2, inset). The selenium atom (^{77}Se, $I = {}^1/_2$, abundance 7.6%) in **4** gave rise to satellites in the ^{195}Pt spectrum due to $^1J(Pt^1Se)$ = 460 Hz but $^1J(Pt^2Se)$ was not resolved.

The FAB mass spectra of the complex cations gave parent ions (envelopes with the expected intensities due to the many isotopomers present) or peaks corresponding to P − H^+ or loss of the terminal ligand on M^1, and this is a very useful method for preliminary characterization of these cationic cluster complexes.

Evidence for Inversion of the Complexes. For the pyramidal structures for **3–7**, the $C^1H^aH^b$ and $C^2H^aH^b$ protons of the dppm

(19) Brown, M. P.; Franklin, S. J.; Puddephatt, R. J.; Thomson, M. A.; Seddon, K. R. *J. Organomet. Chem.* **1979**, *178*, 281.

(20) Grossel, M. C.; Batson, J. R.; Moulding, R. P.; Seddon, K. R. *J. Organomet. Chem.* **1986**, *304*, 391 and references therein.

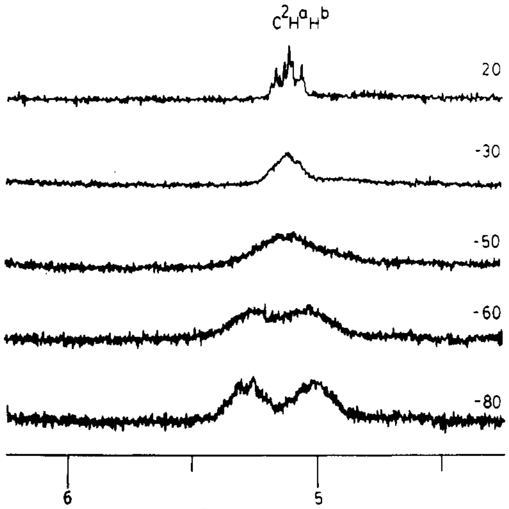

Figure 3. Variable-temperature ^1H NMR spectra (200 MHz) of $[Pd_3(\mu_3\text{-}S)SH(\mu\text{-dppm})_3][PF_6]$, showing only the resonance due to the $C^2H^aH^b$ protons.

methylene groups should be nonequivalent. At low temperatures this was observed, but at room temperature, single resonances were usually observed (Figure 3). This is due to inversion at sulfur of the $M_3(\mu_3\text{-}S)$ groups, which leads to an effective plane of symmetry containing the $M_3(\mu\text{-dppm})_3$ unit, as found previously for $[Pd_3(CN)(\mu_3\text{-}S)(\mu\text{-dppm})_3]^+$.[16] The activation energies calculated by using the Eyring equation are given in Table II. Comparison of the $\Delta G^{\ddagger}$ values for $[M_3H(\mu_3\text{-}S)(\mu\text{-dppm})_3]^+$ shows that inversion is easier when M = Pd than when M = Pt, and for $[Pt_3H(\mu_3\text{-}E)(\mu\text{-dppm})_3]^+$ inversion is easier when E = S than when E = Se. The selenium complex did not undergo detectable inversion at temperatures up to 50 °C, above which decomposition began. These trends are expected by analogy with similar observations on sulfur or selenium inversion in mononuclear and binuclear complexes containing $M\text{-}ER_2$ or $M_2(\mu\text{-}ER)$ groups.[21] However, increasing the trans influence of X in groups $X\text{-}M\text{-}SR_2$ usually leads to a marked reduction in the activation energy for inversion at sulfur,[21] whereas we find that increasing the trans influence of X in $[Pd_3X(\mu_3\text{-}S)(\mu\text{-dppm})_3]^+$ leads to a slight increase in $\Delta G^{\ddagger}$ for inversion of the $Pd_3(\mu_3\text{-}S)$ group (Table II). It is possible that the usual series is reversed because the longer $Pd^1\text{-}S$ bond, when trans to a ligand such as hydride, leads to a greater Pd^1Pd^2 distance in the planar $Pd_3(\mu_3\text{-}S)$ transition state and hence to greater strain in the μ-dppm ligands that bridge the Pd^1Pd^2 edges. A similar effect might be expected to give a larger than usual difference[21] in $\Delta G^{\ddagger}$ values for inversion of the $Pt_3(\mu_3\text{-}E)$ units in **3** and **4** due to the longer Pt–Se bonds in **4**,[22,23] but this could not be determined experimentally.

Structure Description. The structure of **3b** deduced spectroscopically was verified by X-ray crystallographic methods. The crystals are built up from independent ions, and the closest cation–anion distance of approach is 2.38 Å between HC(136) and HC(63) at (1 + *x*, 1 + *y*, *z*). Selected bond distances and angles are given in Table III.

The cation (Figure 4) consists of a triangle of platinum atoms linked by dppm ligands and a triply bridging sulfur atom. This trinuclear cluster contains only one metal–metal bond. The Pt(1)–Pt(3) distance of 2.597 (4) Å is typical of a Pt–Pt single bond. The other Pt···Pt distances, Pt(1)···Pt(2) and Pt(2)···Pt(3), are 3.574 (2) and 3.678 (7) Å, respectively, clearly indicating nonbonding interactions. This is verified spectroscopically as no Pt–Pt coupling involving Pt(2) is observed.

Table III. Intramolecular Bond Distances (Å) and Bond Angles (deg)

Distances			
Pt(1)–Pt(2)	3.574 (2)	Pt(1)–Pt(3)	2.597 (4)
Pt(2)–Pt(3)	3.678 (7)	S–Pt(1)	2.294 (5)
S–Pt(2)	2.375 (6)	S–Pt(3)	2.311 (3)
Pt(1)–P(1)	2.234 (3)	Pt(1)–P(2)	2.258 (3)
Pt(2)–P(3)	2.290 (4)	Pt(2)–P(4)	2.289 (5)
Pt(3)–P(5)	2.272 (6)	Pt(3)–P(6)	2.244 (3)
C(1)–P(1)	1.850 (10)	C(1)–P(6)	1.852 (11)
C(2)–P(2)	1.844 (10)	C(2)–P(3)	1.846 (10)
C(3)–P(4)	1.841 (10)	C(3)–P(5)	1.862 (10)
H–Pt(2)	2.15 (8)		
Angles			
Pt(2)–Pt(1)–Pt(3)	71.2 (2)	Pt(1)–Pt(2)–Pt(3)	41.94 (11)
H–Pt(2)–P(4)	87 (2)	H–Pt(2)–P(3)	83 (2)
H–Pt(2)–S	179 (2)		
Pt(1)–Pt(3)–Pt(2)	66.90 (13)	Pt(3)–Pt(1)–S	55.96 (14)
Pt(3)–Pt(1)–P(1)	91.78 (15)	Pt(3)–Pt(1)–P(2)	155.66 (7)
S–Pt(1)–P(1)	147.72 (10)	S–Pt(1)–P(2)	99.7 (2)
P(1)–Pt(1)–P(2)	112.5 (2)	S–Pt(2)–P(3)	95.4 (2)
S–Pt(2)–P(4)	93.7 (2)	P(3)–Pt(2)–P(4)	168.0 (1)
Pt(1)–Pt(3)–S	55.36 (8)	Pt(1)–Pt(3)–P(5)	151.81 (10)
Pt(1)–Pt(3)–P(6)	97.3 (2)	S–Pt(3)–P(5)	96.50 (10)
S–Pt(3)–P(6)	149.27 (13)	P(5)–Pt(3)–P(6)	110.39 (13)
Pt(1)–S–Pt(2)	99.89 (14)	Pt(1)–S–Pt(3)	68.68 (11)
Pt(2)–S–Pt(3)	103.42 (15)	Pt(1)–P(1)–C(1)	108.6 (3)
Pt(1)–P(2)–C(2)	111.5 (4)	Pt(2)–P(3)–C(2)	118.6 (3)
Pt(2)–P(4)–C(3)	115.7 (3)	P(1)–C(1)–P(6)	108.1 (5)
Pt(3)–P(5)–C(3)	109.3 (3)	P(2)–C(2)–P(3)	116.8 (5)
Pt(3)–P(6)–C(1)	109.3 (3)	P(4)–C(3)–P(5)	114.7 (5)

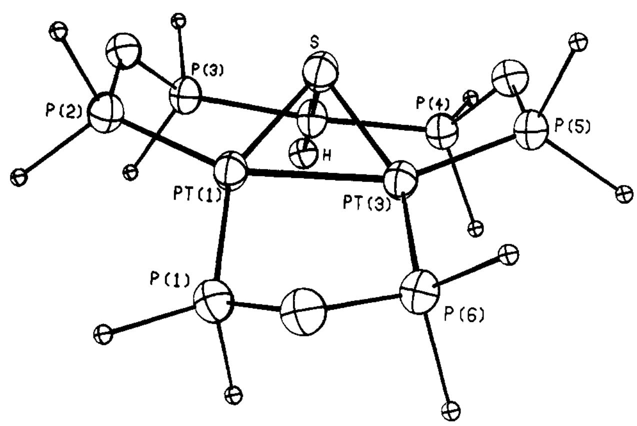

Figure 4. Cluster framework of the cations of **3**. Only the ipso C atoms of the phenyl rings have been included. Atoms are drawn as 50% probability thermal ellipsoids.

Distorted-square-planar geometry is seen at each platinum center. The distortion is most severe around Pt(1) and Pt(3) as the "trans" ligands are significantly removed from linearity (Table III). The Pt(2) center is more regular with a P(3)–Pt(2)–P(4) angle of 168.0 (1)° and a S–Pt(2)–H angle of 179 (2)°. The hydride ligand was readily located in a difference Fourier synthesis, and positional parameters were successfully refined. The final Pt(2)–H distance is 2.15 (8) Å. A search of the 1986 release of the Cambridge data base[24] found 34 entries containing Pt–H bonds, with distances ranging from 1.40 to 2.05 Å. Accurate values of Pt–H(terminal) = 1.610 (2) Å, and Pt–H(bridging) = 1.860 (2), 2.049 (2), 1.691 (2) and 1.656 (2) Å were determined by Koetzle et al.[25] in a neutron diffraction study of the binuclear platinum hydride complex $[H_3Pt_2(Ph_2PCH_2CH_2PPh_2)_2]BPh_4$, whereas Furlani et al.[26] obtained a Pt–H(terminal) distance of

(21) For a review see: Abel, E. W.; Bhargava, S. K.; Orrell, K. G. *Prog. Inorg. Chem.* **1984**, *32*, 1.
(22) Ebner, M.; Otto, H.; Werner, H. *Angew. Chem., Int. Ed. Engl.* **1985**, *24*, 518.
(23) Barnes, J. C.; Hunter, G.; Lown, M. W. *J. Chem. Soc., Dalton Trans.* **1977**, 458.
(24) "Cambridge Crystallographic Database"; University Chemical Laboratory, Cambridge, England, 1986 release.
(25) Chiang, M. Y.; Bau, R.; Minghetti, G.; Bandini, A. L.; Banditelli, G.; Koetzle, T. F. *Inorg. Chem.* **1984**, *23*, 124.
(26) Furlani, A.; Licoccia, S.; Russo, M. V.; Villa, A. C.; Guastini, C. *J. Chem. Soc., Dalton Trans.* **1982**, 2449.

1.98 Å in *trans*-[Pt(C≡CC(OH)MeEt)H{PPh_3}$_2$]. The value found in this study is undoubtedly long by comparison and must be viewed with caution until neutron data can be measured.

The sulfur bridge has a significantly longer bond length to Pt(2) (2.375 (6) Å) than to Pt(1) and Pt(3) (2.294 (5) and 2.311 (3) Å, respectively). This is to be expected from the greater trans influence exhibited by a hydride ligand. These bond lengths are only slightly longer than the Pt–S distance of 2.28 (3) Å obtained from the Pt(111)–S structure. This value was estimated from the vertical Pt–S layer spacing of 1.62 Å determined by LEED, assuming the Pt–Pt distances were not affected by sulfur adsorption. If, however, some lengthening of the Pt–Pt distance occurs as a result of adsorption, as this model **3b** suggests, then even closer agreement in Pt–S bond lengths might be obtained.

Conclusions

The reactions of H_2S with **1** clearly resemble the reaction of H_2S on Pt(111) to give H_2 and $Pt_3(\mu_3\text{-}S)$ groups on the surface.[1–9] We suggest that the initial reaction with **1** occurs by oxidative addition to give $[Pt_3H(\mu_3\text{-SH})(\mu\text{-dppm})_3]^{2+}$ and that rapid deprotonation of the μ_3-SH group then occurs. On the Pt(111) surface, oxidative addition gives chemisorbed H and SH groups that then eliminate H_2. A similar reaction of H_2E with $[Pd_2Cl_2(\mu\text{-dppm})_2]$ gives H_2 and $[Pd_2Cl_2(\mu\text{-E})(\mu\text{-dppm})_2]$, E = S or Se.[27,28] This reaction leads to cleavage of the Pd–Pd bond of $[Pd_2Cl_2(\mu\text{-dppm})_2]$, and the reaction of H_2S with **1** or **2** leads to cleavage of two of the M–M bonds of the parent cluster. However, formation of $Pt_3(\mu_3\text{-}S)$ units on the Pt(111) surface does not appear to cause significant increases in the PtPt distances.[9] Of course, the metal atoms on a surface are anchored much more tightly than in **1** by the underlying atoms, and there is a greater degree of coordinative unsaturation of the surface metal atoms than the metal atoms in **1**.[13] Either or both of these factors could contribute to this difference between the model systems and the metal surface. Nevertheless, these simple model systems mimic many of the features of the surface reactions including, for example, the ease of reaction and the displacement of less strongly bound groups (CO in complex **1**) by the sulfur groups of H_2S.

Experimental Section

NMR spectra were recorded with Varian XL200 (^{1}H) and XL300 (^{31}P{^{1}H} and ^{195}Pt{^{1}H}) spectrometers using acetone-d_6 as solvent. Chemical shifts are quoted with respect to Me_4Si (^{1}H), phosphoric acid (^{31}P), or aqueous K_2PtCl_4 (^{195}Pt). IR spectra were recorded on a Bruker IR/32 FTIR spectrometer, and FAB mass spectra were recorded on a Finnigan MAT 8230 mass spectrometer on mulls in oxalic acid/3-mercapto-1,2-propanediol. Elemental analyses were carried out by Guelph Chemical Laboratories. Complexes **1** and **2** were prepared as described elsewhere.[10,11]

$[Pt_3(\mu\text{-dppm})_3(\mu_3\text{-S})H][PF_6]$ (3). Complex **1** (0.0533 g) was dissolved in acetone (25 mL), and a slow flow of hydrogen sulfide was passed through the solution. The reaction was accompanied by a color change from orange to yellow. Solvent was then removed on the rotary evaporator. The product was washed with ether, giving a yellow crystalline solid in 98% yield. Anal. Calcd for $C_{75}H_{67}P_7F_6SPt_3$: C, 47.00; H, 3.52. Found: C, 47.17; H, 3.72. Mp: 275 °C dec. IR (Nujol): ν(PtH) = 2089 cm^{-1}. MS: calcd for $[Pt_3(\mu\text{-dppm})_3(\mu_3\text{-S})H]^+$, m/e 1771; found, m/e 1770 (P – H).

$[Pt_3(\mu\text{-dppm})_3(\mu_3\text{-S})H][BPh_4]$ (3b). To a solution of **3** (0.0462 g) in acetone (3 mL) was added dropwise a solution of $NaBPh_4$ (0.0521 g) in methanol (2 mL). Water (2.5 mL) was added to precipitate the product. Filtering afforded a yellow product, spectroscopically pure, from which single crystals were grown.

$[Pt_3(\mu\text{-dppm})_3(\mu_3\text{-Se})H][PF_6]$ (4). Hydrogen selenide, prepared in situ by reaction of Na_2Se (0.03 g) with H_2SO_4 (20 mL, 2 M) at 0 °C, was bubbled through a solution of **1** (0.0938 g) in acetone (40 mL) turning the orange solution yellow. Evaporation under reduced pressure gave an orange solid. This was washed with cold acetone, giving a yellow solid in 83% yield. Anal. Calcd for $C_{75}H_{67}P_7F_6SePt_3$: C, 45.88; H, 3.44. Found: C, 45.11; H, 3.52. Mp: 290 °C dec. IR (Nujol): ν(PtH) = 2105 cm^{-1}. MS: calcd for $[Pt_3(\mu\text{-dppm})_3(\mu_3\text{-Se})H]^+$, m/e 1818; found, m/e 1818.

$[Pd_3(\mu\text{-dppm})_3(\mu_3\text{-S})H][PF_6]$ (5). In a Schlenk tube complex **2** (0.0514 g) was dissolved in acetone (10 mL) at –78 °C. The air was evacuated and an atmosphere of hydrogen sulfide was admitted. The deep purple solution turned clear red. Excess hydrogen sulfide and acetone were removed under reduced pressure at 0 °C. A red crystalline powder, **5**, was obtained in 97% yield. This complex decomposed in the solid state, and satisfactory analytical data could not be obtained: mp 205 °C dec. IR (Nujol): ν(PdH) = 1910 cm^{-1}. MS: calcd for $[Pd_3(\mu\text{-dppm})_3(\mu_3\text{-S})H]^+$, m/e 1505; found, m/e 1504 (P – H).

$[Pd_3(\mu\text{-dppm})_3(\mu_3\text{-S})(SH)][PF_6]$ (6). Hydrogen sulfide was bubbled through a solution of complex **2** (0.0630 g) in acetone (20 mL). The resulting solution was left to react for 60 min at ambient temperature under an atmosphere of hydrogen sulfide gas. Nitrogen gas was bubbled through the solution to reduce the volume, and pentane was layered, giving a red microcrystalline solid after 16 h; mp 190 °C, dec. at 130 °C. MS: calcd for $[Pd_3(\mu_3\text{-S})SH(\mu\text{-dppm})_3]^+$, m/e 1537; found, m/e 1504 (P – SH).

$[Pd_3(\mu\text{-dppm})_3(\mu_3\text{-S})Cl][PF_6]$ (7). Compound **5** (0.0537 g) was dissolved in chloroform (10 mL) and left to stir for 20 h. The reaction solution was evaporated under reduced pressure and washed with ether. This gave a red solid in 90% yield; mp 208 °C dec. MS: calcd for $[Pd_3(\mu_3\text{-S})Cl(\mu\text{-dppm})_3]^+$, m/e 1539; found, m/e 1504 (P – Cl).

Collection and Reduction of X-ray Data. Transparent yellow prisms were grown by slow diffusion of pentane into an acetone solution of **3b**. Preliminary photography revealed monoclinic symmetry, and the systematic absences unambiguously indicated space group $P2_1/c$, No. 14.[29]

Table IV. Summary of X-ray Structure Determination

Crystal Data	
compd; M_R	$C_{99}H_{87}BP_6Pt_3S$; 2090.8
cryst syst; space group	monoclinic; $P2_1/c$
syst absences	$h0l$, l odd; $0k0$, k odd
cell dimens at 21 °C: a, b, c, Å; β, deg	11.338 (1), 17.303 (2), 42.957 (3); 90.30 (1)
cell vol, Å^3; Z	8428 (2); 4
d, g cm^{-3}: obsd; calcd	1.65 (1); 1.648
Experimental Data	
diffractometer	Enraf-Nonius CAD4F
prefilter	Ni foil, 0.015 mm
radiation; wavelength, Å	Cu; λ(Cu K$\bar{\alpha}$) 1.541 84
cryst–detec, mm; toa, deg	205; 2.5
aperture, mm: vert; horiz	4; 0.50 + 0.15 tan θ
no. of centering reflcns; θ range, deg	20; $22 \le \theta \le 28$
Data Collection	
approx cryst dimens, mm	0.13 × 0.15 × 0.19
cryst vol, mm^3; no. of faces	2.66 × 10^{-3}; 8
face indices	{001}, {012}, 301, cut face $\bar{4}1\bar{2}$
ω-scan widths, deg: before; after	0.12; 0.13
scan mode; width, deg	ω–2θ; 0.7 + 0.35 tan θ
index; θ range, deg	$0 \le h \le 12$, $-18 \le k \le 0$, $-45 \le l \le 45$; $0 \le \theta \le 55$
scan speed, deg min^{-1}	1.3–3.4
max time/datum, s; total time, h	75; 200
std reflcns	$1\bar{1}0$, 300, $0\bar{2}0$, 004
monitor frequency, % var	3 h; random
no. of data; no. of stds colled	12 085; 304
Data Processing	
cor	Lorentz and polarization
decay; abs cor	none; Gaussian
abs coeff, mm^{-1}; grid size	10.91; 14 × 12 × 10
transmissn: max; min	0.369; 0.264
$R(F)$ for av: before; after	0.013; 0.013
no. of unique data; signif	9398, $I > 0$
Structure Refinement	
no. of observns; no. of variables	8258 with $I > 3\sigma(I)$; 303
final model: R_1; R_2	0.0429; 0.0420
extinction param	4.8 (1) × 10^{-7}
top residual, e Å^{-3}; coord	0.9 (1); 0.107, 0.046, –0.070
largest shift, param	0.21σ for y of H, all others <0.1σ
statistical analysis	no unusual trends

(27) Lee, C.-L.; Besenyi, G.; James, B. R.; Nelson, D. A.; Lilga, M. A. *J. Chem. Soc., Chem. Commun.* **1985**, 1175.

(28) Besenyi, G.; Lee, C.-L.; James, B. R. *J. Chem. Soc., Chem. Commun.* **1986**, 1750.

(29) *International Tables for X-ray Crystallography*; Kynoch: Birmingham, England: 1969, Vol. I; 1974, Vol. IV.

Table V. Atomic Positional (×10[4]) and Thermal (Å[2] × 10[3]) Parameters

atom	x	y	z	U or U_{eq}[a]	atom	x	y	z	U or U_{eq}[a]
Pt(1)	−38.4 (4)	2200.2 (2)	5987.98 (10)	34.4 (3)	C(76)	−6222 (6)	1634 (4)	6354 (1)	52 (3)
Pt(2)	−2995.5 (4)	1510.6 (3)	6060.44 (10)	37.9 (3)	C(81)	−4333 (6)	2890 (3)	6529 (2)	41 (3)
Pt(3)	−835.2 (4)	2586.4 (2)	6532.10 (10)	33.9 (3)	C(82)	−5060 (6)	3137 (4)	6770 (1)	52 (3)
S	−1115 (2)	1394 (1)	6301 (1)	40 (2)	C(83)	−5421 (6)	3905 (4)	6784 (2)	65 (4)
P(1)	823 (3)	3351 (2)	5927 (1)	42 (2)	C(84)	−5054 (7)	4426 (3)	6557 (2)	75 (4)
P(2)	267 (2)	1404 (2)	5580 (1)	38 (2)	C(85)	−4327 (7)	4179 (4)	6317 (2)	72 (4)
P(3)	−2430 (2)	992 (2)	5594 (1)	39 (2)	C(86)	−3966 (6)	3411 (4)	6303 (1)	59 (3)
P(4)	−3910 (2)	1877 (2)	6511 (1)	38 (2)	C(91)	−966 (5)	1819 (4)	7245 (1)	41 (3)
P(5)	−1888 (2)	2336 (2)	6969 (1)	38 (2)	C(92)	−494 (6)	1107 (4)	7161 (1)	56 (3)
P(6)	282 (2)	3645 (2)	6599 (1)	40 (2)	C(93)	303 (6)	735 (3)	7357 (2)	73 (4)
C(1)	1469 (9)	3653 (6)	6304 (2)	43 (3)	C(94)	627 (6)	1075 (4)	7639 (2)	68 (4)
C(2)	−893 (8)	660 (5)	5551 (2)	37 (3)	C(95)	155 (7)	1787 (4)	7723 (1)	65 (4)
C(3)	−3108 (8)	1655 (6)	6874 (2)	38 (3)	C(96)	−641 (6)	2159 (3)	7526 (2)	53 (3)
B	4126 (11)	7230 (8)	6508 (3)	51 (4)	C(101)	−2650 (6)	3046 (4)	7211 (1)	37 (3)
H	−4686 (70)	1607 (47)	5833 (18)	51	C(102)	−2446 (6)	3830 (4)	7162 (1)	58 (3)
C(11)	2068 (7)	3491 (5)	5664 (2)	46 (3)	C(103)	−3055 (7)	4379 (3)	7335 (2)	80 (4)
C(12)	3152 (9)	3170 (5)	5745 (2)	94 (5)	C(104)	−3868 (6)	4143 (4)	7558 (2)	69 (4)
C(13)	4100 (6)	3222 (6)	5542 (3)	130 (6)	C(105)	−4072 (6)	3360 (5)	7607 (1)	63 (3)
C(14)	3964 (8)	3595 (6)	5257 (2)	120 (6)	C(106)	−3463 (6)	2811 (3)	7434 (2)	54 (3)
C(15)	2880 (10)	3916 (5)	5175 (2)	117 (6)	C(111)	1102 (6)	3571 (4)	6965 (1)	41 (3)
C(16)	1932 (7)	3864 (5)	5379 (2)	79 (4)	C(112)	1799 (7)	2916 (4)	7007 (2)	60 (3)
C(21)	−175 (6)	4123 (4)	5812 (2)	49 (3)	C(113)	2402 (6)	2806 (4)	7286 (2)	72 (4)
C(22)	196 (6)	4890 (5)	5808 (2)	72 (4)	C(114)	2309 (7)	3351 (5)	7524 (1)	74 (4)
C(23)	−586 (9)	5472 (3)	5721 (2)	95 (5)	C(115)	1612 (7)	4005 (4)	7481 (1)	77 (4)
C(24)	−1740 (8)	5287 (5)	5637 (2)	99 (5)	C(116)	1009 (6)	4115 (3)	7202 (2)	62 (3)
C(25)	−2111 (5)	4520 (6)	5641 (2)	95 (5)	C(121)	−274 (6)	4636 (3)	6572 (2)	41 (3)
C(26)	−1329 (7)	3938 (4)	5728 (2)	63 (3)	C(122)	−1466 (6)	4761 (4)	6511 (2)	53 (3)
C(31)	1594 (5)	826 (4)	5635 (2)	41 (3)	C(123)	−1880 (5)	5509 (5)	6462 (2)	73 (4)
C(32)	1601 (6)	167 (4)	5820 (2)	65 (4)	C(124)	−1102 (7)	6131 (3)	6473 (2)	74 (4)
C(33)	2664 (8)	−194 (4)	5893 (2)	83 (4)	C(125)	90 (6)	6005 (4)	6533 (2)	64 (4)
C(34)	3719 (6)	103 (5)	5780 (2)	78 (4)	C(126)	503 (4)	5258 (4)	6583 (2)	52 (3)
C(35)	3712 (5)	762 (5)	5595 (2)	76 (4)	C(131)	4374 (7)	6645 (4)	6196 (1)	58 (3)
C(36)	2649 (7)	1124 (4)	5522 (2)	67 (4)	C(132)	3653 (6)	6002 (5)	6156 (2)	80 (4)
C(41)	375 (6)	1763 (4)	5185 (1)	39 (3)	C(133)	3772 (7)	5542 (4)	5892 (2)	92 (5)
C(42)	825 (6)	1301 (3)	4948 (2)	51 (3)	C(134)	4612 (8)	5727 (5)	5668 (2)	79 (4)
C(43)	940 (6)	1598 (4)	4649 (1)	70 (4)	C(135)	5333 (7)	6371 (5)	5709 (2)	80 (4)
C(44)	606 (7)	2356 (5)	4586 (1)	74 (4)	C(136)	5214 (7)	6830 (4)	5973 (2)	74 (4)
C(45)	156 (7)	2818 (3)	4823 (2)	86 (4)	C(141)	4117 (7)	6672 (4)	6837 (1)	55 (3)
C(46)	41 (6)	2521 (4)	5122 (2)	61 (3)	C(142)	3050 (5)	6319 (5)	6910 (2)	68 (4)
C(51)	−2681 (6)	1563 (4)	5247 (1)	42 (3)	C(143)	2973 (5)	5835 (4)	7168 (2)	69 (4)
C(52)	−3085 (6)	2316 (4)	5288 (1)	60 (3)	C(144)	3964 (7)	5705 (4)	7353 (1)	67 (4)
C(53)	−3225 (7)	2800 (3)	5031 (2)	86 (4)	C(145)	5030 (6)	6057 (5)	7281 (2)	70 (4)
C(54)	−2961 (7)	2532 (4)	4734 (2)	80 (4)	C(146)	5107 (5)	6541 (4)	7023 (2)	62 (3)
C(55)	−2557 (7)	1779 (5)	4694 (1)	68 (4)	C(151)	2821 (6)	7665 (4)	6462 (2)	57 (3)
C(56)	−2417 (6)	1295 (3)	4950 (2)	52 (3)	C(152)	2262 (8)	7685 (5)	6173 (2)	78 (4)
C(61)	−3162 (6)	56 (3)	5544 (2)	38 (3)	C(153)	1186 (8)	8063 (5)	6139 (2)	95 (5)
C(62)	−3127 (6)	−423 (4)	5804 (1)	52 (3)	C(154)	669 (6)	8423 (5)	6394 (2)	91 (5)
C(63)	−3619 (7)	−1159 (4)	5790 (1)	62 (3)	C(155)	1227 (8)	8403 (5)	6683 (2)	100 (5)
C(64)	−4145 (6)	−1417 (3)	5516 (2)	61 (3)	C(156)	2303 (8)	8025 (5)	6717 (1)	82 (4)
C(65)	−4179 (6)	−938 (4)	5255 (1)	55 (3)	C(161)	5232 (6)	7897 (4)	6542 (2)	49 (3)
C(66)	−3687 (6)	−202 (4)	5269 (1)	50 (3)	C(162)	4979 (5)	8682 (5)	6565 (2)	66 (4)
C(71)	−5357 (4)	1428 (4)	6569 (2)	35 (3)	C(163)	5890 (8)	9214 (3)	6601 (2)	78 (4)
C(72)	−5645 (6)	962 (4)	6822 (1)	64 (3)	C(164)	7054 (6)	8961 (4)	6614 (2)	78 (4)
C(73)	−6798 (7)	702 (4)	6859 (2)	86 (4)	C(165)	7308 (5)	8176 (5)	6591 (2)	75 (4)
C(74)	−7663 (5)	909 (5)	6643 (2)	72 (4)	C(166)	6396 (7)	7644 (3)	6555 (2)	61 (3)
C(75)	−7375 (5)	1375 (4)	6391 (2)	61 (3)					

[a] $U_{eq} = {}^1/_3\sum_i\sum_j U_{ij}a_i^*a_j^*\mathbf{a}_i\cdot\mathbf{a}_j$.

The density was determined by neutral buoyancy in a mixture of 1,2-dibromoethane and pentane.

The crystal was mounted in air and an orientation matrix and cell dimensions were determined at $\pm\theta$ from high-angle reflections on an Enraf-Nonius CAD4F diffractometer.[30] Crystal data and experimental details are found in Table IV. Intensity data were collected by the θ–2θ scan technique at room temperature. ω scans of several intense reflections had average widths at half-height of 0.12 and 0.13° before and after data collection, respectively. Background and Lorentz and polarization corrections were applied and standard deviations assigned.[31] The data were corrected for absorption, and 590 symmetry-equivalent reflections were averaged (R (on F) = 0.013) to give 9398 unique reflections with $I > 0$ for the analysis.

Structure Solution and Refinement. The structure was solved by Patterson/Fourier methods and refined by full-matrix least squares on F, minimizing the function $\sum w(|F_o| - |F_c|)^2$, where the weight w is given by $4|F_o|/\sigma^2(F_o)^2$. Scattering factors for neutral, non-hydrogen atoms and the real parts of the anomalous dispersion correction were taken from ref 29, while H atom scattering factors were taken from Stewart et al.[32] Only the Pt, P, and S atoms were assigned anisotropic thermal parameters. Once all the non-hydrogen atoms had been located, the structure was transferred to the UWO suite of programs[33] to complete the refinement. The 16 phenyl rings were constrained[34] to D_{6h} geometry (C–C =

(30) *Enraf-Nonius CAD4F Users Manual*; Enraf-Nonius Delft: Delft, The Netherlands, 1984.

(31) "Enraf-Nonius Structure Determination Package, SDP-PLUS", Version 1.1; Enraf-Nonius Delft, Delft, The Netherlands, 1984.

(32) Stewart, R. F.; Davidson, E. R.; Simpson, W. T. *J. Chem. Phys.* **1965**, *42*, 3175.

(33) Programs used included local modifications for the CDC Cyber 170-835 at the University of Western Ontario of the following: full-matrix least squares, J. A. Ibers' NUCLS; Fourier syntheses, A. Zalkin's FORDAP; functions and errors, W. R. Busing, K. O. Martin, and H. A. Levy's ORFFE; illustrations, C. K. Johnson's ORTEPII.

1.392 Å) and refined with individual isotropic thermal parameters for the ring C atoms. Convergence occurred at $R_1 = \sum||F_o| - |F_c||/\sum|F_o| = 0.049$ and $R_2 = (\sum w(|F_o| - |F_c|)^2/(\sum|F_o|^2))^{1/2} = 0.053$.

All 87 H atoms were located in positive electron density in a difference Fourier synthesis ((sin θ)/λ maximum 0.35) with 77 of them appearing as distinct peaks with densities varying from 0.3 (1) to 0.6 (1) e $Å^{-3}$. All but the hydride atom were included in idealized positions (sp^2, C–H = 0.90 Å; sp^3, C–H = 0.95 Å) with thermal parameters set at 110% of that of the atom to which they are bonded. Their positions were updated as the refinement progressed, but they were not refined. There was evidence for secondary extinction, and a correction was included.[35] Following our preliminary report,[17] a successful attempt was made to refine the hydride atom positional parameters. The final cycles of refinement included 303 variables, 8258 unique observations, and a p value of 0.04 and converged at agreement factors of $R_1 = 0.0429$ and $R_2 = 0.0420$ and a goodness-of-fit value of 2.50e. The largest parameter shift in the final cycle was 0.21σ, associated with the y coordinate of the hydride atom. The highest residual electron density was 0.9 (1) e $Å^{-3}$ at (0.107, 0.046, –0.070), near C(23) and C(24) and was of no chemical significance. A statistical analysis on $|F_o|$, λ^{-1} sin θ, and various combinations of Miller indices and diffractometer setting angles showed no unusual trends and indicated a satisfactory weighting scheme.

Atomic positional and U_{eq} or U thermal parameters are listed in Table V. Additional crystallographic data are included as supplementary material.[36]

Acknowledgment. We thank the NSERC (Canada) for financial support (N.C.P., R.J.P.) and for a graduate fellowship (M.C.J.).

Registry No. 1, 99642-80-5; 2, 89189-82-2; 3, 107206-14-4; 3b, 107207-51-2; 4, 110433-38-0; 5, 110433-44-8; 6, 110433-42-6; 7, 110433-40-4; S, 7704-34-9; Se, 7782-49-2; chloroform, 67-66-3.

Supplementary Material Available: Tables SI–SV, listing derived hydrogen atom parameters, rigid-group parameters, anisotropic thermal parameters, angles and distances associated with the phenyl rings, and a weighted least-squares plane and selected torsion angles (8 pages); a table of observed and calculated structure amplitudes (37 pages). Ordering information is given on any current masthead page.

(34) Eisenberg, R.; Ibers, J. A. *Inorg. Chem.* **1965**, *4*, 773.
(35) Zachariasen, W. H. *Acta Crystallogr., Sect. A: Cryst. Phys., Diffr. Theor. Gen. Crystallogr.* **1968**, *A24*, 212–216.
(36) See paragraph describing supplementary material at the end of the paper.

Contribution from the Department of Chemistry and Molecular Structure Center, Indiana University, Bloomington, Indiana 47405

1,2-Bis(di-*tert*-butylarsenido)tetrakis(dimethylamido)dimolybdenum and -ditungsten. Synthesis, Structures, and Solution Behavior

M. H. Chisholm,* J. C. Huffman, and J. W. Pasterczyk

Received May 27, 1987

The compounds 1,2-$M_2(As\text{-}t\text{-}Bu_2)_2(NMe_2)_4$ (M = Mo, W) are obtained as hydrocarbon-soluble crystalline solids in the reaction between 1,2-$M_2Cl_2(NMe_2)_4$ and 2 equiv of LiAs-t-Bu_2 in THF at –78 °C. Both are light-sensitive in solution; the molybdenum compound sublimes at 95 °C (10^{-4} Torr). X-ray crystal structure determinations revealed that both compounds crystallize in the anti rotameric form of the familiar 1,2-disubstituted ethane-like configuration for $X_2YM{\equiv}MX_2Y$. The metal–metal distances (2.2159 (12) Å for M = Mo, 2.3001 (11) Å for M = W) are typical for unbridged d^3–d^3 dimers. The geometries about the arsenic atoms are distinctly pyramidal, and those about the nitrogen atoms are planar, with the average M–N distances (1.972 (6) Å for M = Mo, 1.955 (9) Å for M = W) being statistically identical with those found in the corresponding $M_2(NMe_2)_6$ compounds. The Mo–As and W–As distances (2.6163 (11) and 2.5949 (15) Å, respectively) are the first measured M–As distances for a transition-metal compound with a terminal arsenido ligand. The solution behavior of these compounds, as investigated by variable-temperature ^1H NMR spectroscopy, corresponds to 1:1 mixtures of anti and gauche rotamers interconverting slowly on the NMR time scale. Interpretation of these spectra requires rotation about the M–N and M–As bonds, the latter process having a lower energy barrier than the former, as well as rapid inversion of the arsenic atoms. These results indicate considerably more ground-state π-bond character between the metal and nitrogen atoms than between the metal and arsenic atoms. Crystal data for $Mo_2(As\text{-}t\text{-}Bu_2)_2(NMe_2)_4$ at –155 °C: a = 14.841 (3) Å, b = 10.478 (2) Å, c = 10.367 (1) Å, β = 90.84 (1)°, Z = 2, d_{calcd} = 1.538 g cm^{-3}, monoclinic space group $P2_1/n$. Crystal data for $W_2(As\text{-}t\text{-}Bu_2)_2(NMe_2)_4$ at –153 °C: a = 14.795 (5) Å, b = 10.505 (3) Å, c = 10.379 (3) Å, β = 91.14 (2)°, Z = 2, d_{calcd} = 1.899 g cm^{-3}, monoclinic space group $P2_1/n$.

Introduction

The coordination chemistry of the $(Mo{\equiv}Mo)^{6+}$ and $(W{\equiv}W)^{6+}$ units has been the subject of intensive investigation for more than a decade and has continued to yield fascinating results.[1] However, the bulk of this work has been performed for ligands coordinated to the metals by second-row main-group atoms, specifically carbon, nitrogen, and oxygen. Sufficient chemical differences exist between the second-row elements and their heavier congeners,[2] however, to warrant a more thorough investigation of the use of heavy main-group anionic ligands in dinuclear transition-metal chemistry.

Efforts in our laboratories in this vein have heretofore been limited primarily to thiolate[3] and phosphido[4] ligands. A number of reasons make arsenic, in addition, an attractive element to incorporate into an organometallic compound. Weaker metal–arsenic and carbon–arsenic bonds[5] compared to those of its lighter congeners raise the possibility of facile thermolysis or photolysis of compounds whose molecular structures are well-known, possibly affording higher nuclearity clusters via mechanistically interesting routes, or perhaps yielding solid-state materials with unique and useful photochemical, magnetic, or electrical properties. This latter prospect is particularly intriguing considering the current interest

(1) (a) Chisholm, M. H. *Polyhedron* **1983**, *2*, 681. (b) Chisholm, M. H.; Cotton, F. A. *Acc. Chem. Res.* **1978**, *11*, 356. (c) Chisholm, M. H. *Transition Met. Chem.* **1978**, *3*, 321. (d) Chisholm, M. H. *Angew. Chem., Int. Ed. Eng.* **1986**, *25*, 21.
(2) See, e.g.: Greenwood, N. N.; Earnshaw, A. *Chemistry of the Elements*; Pergamon: Oxford, 1984.
(3) Chisholm, M. H.; Corning, J. F.; Folting, K.; Huffman, J. C. *Polyhedron* **1985**, *4*, 383 and references therein.
(4) Buhro, W. E.; Chisholm, M. H.; Folting, K.; Huffman, J. C. *J. Am. Chem.* Soc. **1987**, *109*, 905
(5) Dasent, W. E. *Inorganic Energetics*; Penquin: Harmondsworth, England, 1970.

0020-1669/87/1326-3781$01.50/0